NATIONAL BUREAU OF STANDARDS REPORT

9491

ANNUAL REPORT FOR THE PERIOD ENDING DECEMBER 31, 1966 ON

NBS PROJECT 3120445

INVESTIGATION OF THE DIRECTIONAL EFFECTS IN THE STRESS CORROSION OF ALUMINUM ALLOYS

by

Jerome Kruger
Gilbert M. Ugiansky
S. Wayne Stiefel
and
Hugh L. Logan

for

National Aeronautics and Space Administration
George C. Marshall Space Flight Center
Huntsville, Alabama

Contract H-2151A
Control 1-6-54-01046-01 (1F)

U. S. DEPARTMENT OF COMMERCE
NATIONAL BUREAU OF STANDARDS

THE NATIONAL BUREAU OF STANDARDS

The National Bureau of Standards is a principal focal point in the Federal Government for assuring maximum application of the physical and engineering sciences to the advancement of technology in industry and commerce. Its responsibilities include development and maintenance of the national standards of measurement, and the provisions of means for making measurements consistent with those standards; determination of physical constants and properties of materials; development of methods for testing materials, mechanisms, and structures, and making such tests as may be necessary, particularly for government agencies; cooperation in the establishment of standard practices for incorporation in codes and specifications; advisory service to government agencies on scientific and technical problems; invention and development of devices to serve special needs of the Government; assistance to industry, business, and consumers in the development and acceptance of commercial standards and simplified trade practice recommendations; administration of programs in cooperation with United States business groups and standards organizations for the development of international standards of practice; and maintenance of a clearinghouse for the collection and dissemination of scientific, technical, and engineering information. The scope of the Bureau's activities is suggested in the following listing of its three Institutes and their organizational units.

Institute for Basic Standards. Applied Mathematics. Electricity. Metrology. Mechanics. Heat. Atomic Physics. Physical Chemistry. Laboratory Astrophysics.* Radiation Physics. Radio Standards Laboratory:* Radio Standards Physics; Radio Standards Engineering. Office of Standard Reference Data.

Institute for Materials Research. Analytical Chemistry. Polymers. Metallurgy. Inorganic Materials. Reactor Radiations. Cryogenics.* Materials Evaluation Laboratory. Office of Standard Reference Materials.

Institute for Applied Technology. Building Research. Information Technology. Performance Test Development. Electronic Instrumentation. Textile and Apparel Technology Center. Technical Analysis. Office of Weights and Measures. Office of Engineering Standards. Office of Invention and Innovation. Office of Technical Resources. Clearinghouse for Federal Scientific and Technical Information.**

---

*Located at Boulder, Colorado, 80301.
**Located at 5285 Port Royal Road, Springfield, Virginia, 22171.

NATIONAL BUREAU OF STANDARDS REPORT

NBS PROJECT	December 31, 1966	NBS REPORT
3120445		9491

ANNUAL STATUS REPORT FOR THE PERIOD ENDING 12/31/66

on

INVESTIGATION OF THE DIRECTIONAL EFFECTS IN THE STRESS CORROSION OF ALUMINUM ALLOYS

by

Jerome Kruger
Gilbert M. Ugiansky
S. Wayne Stiefel
and
Hugh L. Logan

for

National Aeronautics and Space Administration
George C. Marshall Space Flight Center
Huntsville, Alabama

Contract H-2151A
Control 1-6-54-01046-01 (1F)

IMPORTANT NOTICE

NATIONAL BUREAU OF STAND ccounting documents intended for use within the Government. Befc ected to additional evaluation and review. For this reason, the pul ng of this Report, either in whole or in part, is not authorized lice of the Director, National Bureau of Standards, Washington 2! Government agency for which the Report has been specifically prep s for its own use.

Approved for public release by the director of the National Institute of Standards and Technology (NIST) on October 9, 2015

U. S. DEPARTMENT OF COMMERCE
NATIONAL BUREAU OF STANDARDS

This report was prepared by the Corrosion Section, National Bureau of Standards under Contract No. H-2151A "Investigation of the Directional Effects in the Stress Corrosion of Aluminum Alloys" for the George C. Marshall Space Flight Center of the National Aeronautics and Space Administration. The work was administered under the technical direction of the Propulsion and Vehicle Engineering Laboratory, Materials Division of the George C. Marshall Space Flight Center with D.B. Franklin acting as project manager.

PROGRAM PLANNING CHART

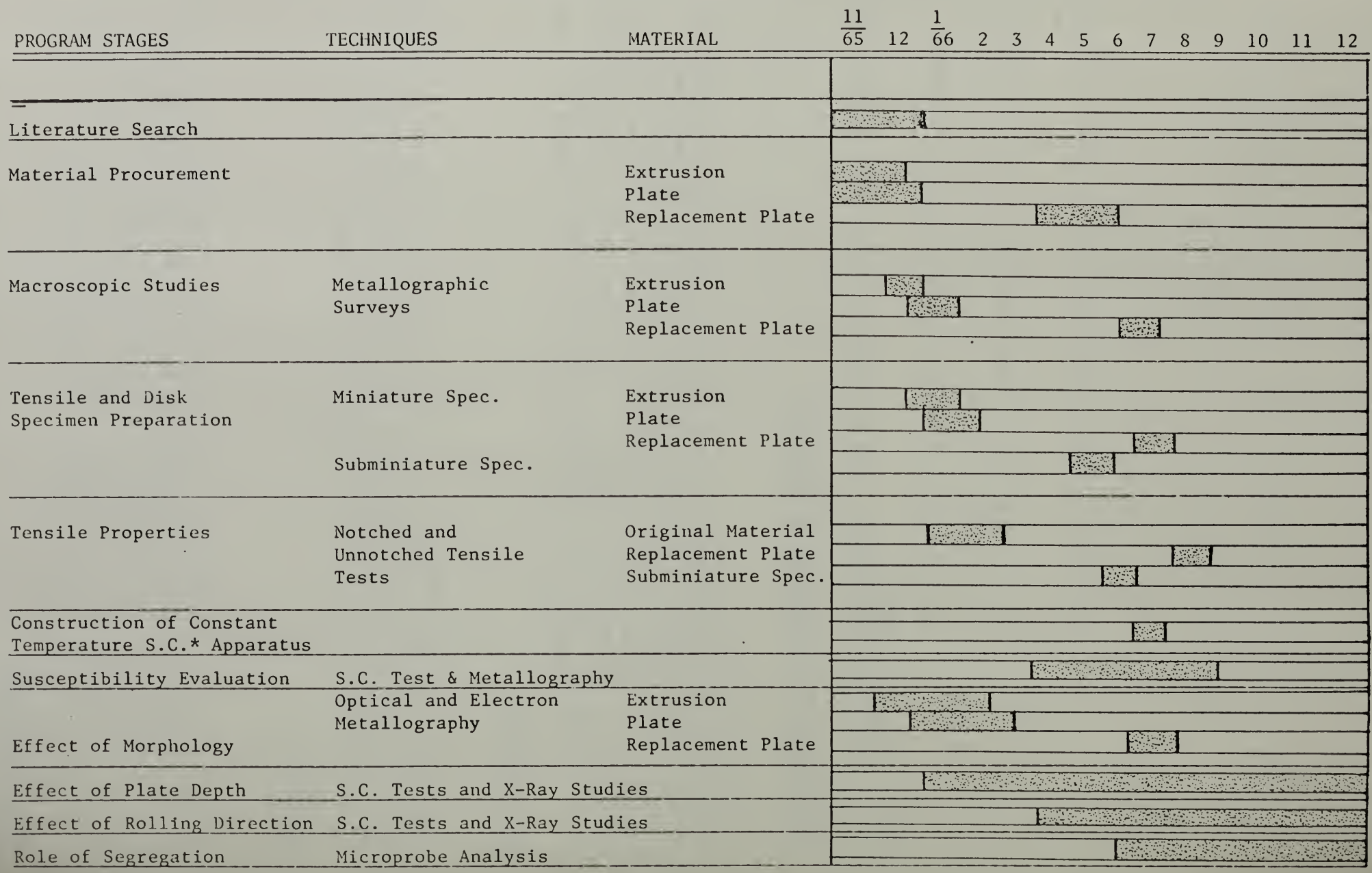

*S.C. - Stress Corrosion

ANTICIPATED WORK

The anticipated work consists of a continuation of the work already started and of new studies designed to determine the directional effects in the stress-corrosion of aluminum alloys. Studies of the roles of preferred orientation and segregation in stress-corrosion of the materials not yet studied will be continued. Work will be initiated to study the effect of grain shape on susceptibility and to study the mechanisms of stress-corrosion by combining electron microscopy techniques and passivity studies.

ABSTRACT

This year's work has been concerned with two areas. The first dealt with confirmation of the expected properties of the received materials. The second concerned investigation of the role of directionality in stress corrosion cracking of aluminum alloys and consisted of studies of preferred orientation and segregation.

WORK PROGRESS

The work accomplished during the first year can be divided into two broad categories. The first included studies to confirm the expected properties of the materials received. The second involved work designed to establish the reasons for the dependence of stress corrosion susceptibility on stress direction in wrought, high strength, aluminum alloys. In this second category, the work consisted of a study of preferred orientation versus susceptibility and a study of the role of segregation in stress corrosion.

CONFIRMATION OF PROPERTIES OF MATERIALS

Material Procurement: The following materials were secured for use in this investigation.

a. Pieces from 3" x 6" extrusions of 7075-T6 aluminum alloy.

b. Pieces from 3" x 6" extrusions of 7075-T73 aluminum alloy.

c. 7075-T651 aluminum alloy plate, 2.5" thick x 2' square.

d. 7075-T73 aluminum alloy plate, 2.5" thick x 2' square.

e. 2219-T37 aluminum alloy plate, 2.4" thick x 2' square.

f. 2219-T87 aluminum alloy plate, 2.4" thick x 2' square.

Delay was encountered due to the manufacturers recall of the 2219 plate material, which was found to be defective. Prior to the recall, considerable work was done on this material. During machining of short transverse specimens from the 2219-T87 plate, three were broken. We attributed this to poor machining technique. However, two notched tensile specimens from a nearby area broke in tensile test not at the notch, but in a region having 9/4 the area at the root of the notch and at a stress computed to be 6100 psi. The location of these fractures was at approximately the same depth below the surface of the plate as those in the specimens broken during machining as shown with a macroetched cross-section of the plate in Figure 1. Adjacent short transverse specimens, one of which was sectioned longitudinally for metallographic examination, were radiographed and showed some indication of voids or inclusions. The metallographic examination confirmed a layer of inclusions or voids.

Structure Studies: Macroscopic examination was made of all materials to determine areas from which specimens were to be removed. Cross-sections of all material were macroetched to show grain flow, as shown for the 7075-T6 extrusion in Figure 2. On the basis of these examinations, all specimens were machined such that the reduced section of the specimen always lay within the center uniform area. The microstructures of all materials were also studied to ensure that the grain shape varied with direction as expected. Figure 3 is a composite photomicrograph showing typical microstructures in three orientations at the interior of the 7075 aluminum alloy received. Changes in microstructure from the surface toward the center of the extrusion in Figure 2 are seen in Figure 4.

Production of Specimens: Both notched and standard round tensile specimens were machined from the extruded material and standard round tensile specimens were also machined from the plate material. Specimens were machined from each material in three orientations with respect to the rolling direction.

Mechanical Testing: Tensile tests were completed for all materials to verify the specified mechanical properties. The yield strength of the materials was used to determine loads in subsequent stress corrosion tests.

Stress Corrosion Testing: Constant temperature apparatus was assembled so that all stress corrosion tests could be carried out at a constant temperature of 35.0 ± 0.1°C. This eliminated the effects of temperature variation on susceptibility. Figure 5 shows the flow of the

recirculating corrosive solution from the constant temperature reservoir and coil to the cell containing the stress corrosion specimen. The system holds approximately 250 ml of solution which is discarded after each specimen is tested. Failure times are recorded to the tenth minute with an interval timer activated by a microswitch placed beneath the weights used to stress the specimen. When the specimen fails, the solution is automatically drained to prevent excessive corrosion of the specimen after failure. Two accelerated stress corrosion test methods were tried. Anodic polarization using a 3 1/2% NaCl solution produced a great amount of overall corrosion with exfoliation. Total immersion of the specimen in Alcoa H solution (0.3% NaCl + 3.0% $K_2Cr_2O_7$ + 3.0% CrO_3 using distilled water, solution pH 0.9) was found to be superior to anodic polarization in 3 1/2% NaCl as an accelerated stress corrosion environment. All stress corrosion tests were run at a constant fraction of the yield strength. The relationship between stress corrosion susceptibility and specimen orientation was established for all materials and found to be as expected.

INVESTIGATION OF THE DIRECTIONAL EFFECTS IN THE STRESS CORROSION OF ALUMINUM ALLOYS

Preferred Orientation Versus Susceptibility of 7075-T651*

Preferred orientation studies were completed on 7075-T651 aluminum alloy plate. Flat disc specimens were machined from various levels in a 2.5 inch thick plate. Pole figures of the (111) reflex were determined for specimens at 0.26, 0.57, 0.73, 0.89, and 1.20 inches below the surface of the plate. These pole figures are shown in Figure 6a through 6e, respectively. The relative intensities shown are an indication of the number of slip planes oriented with their poles at the angles shown on the pole figures.

Role of Depth for a Given Direction: For short transverse stress corrosion specimens, the stress direction is as indicated in Figure 7. The highly susceptible grain boundaries, i.e., those normal to the stress direction, are in the equator plane. If the (111) pole is at an angle of ϕ with the equator plane (grain boundary), then the (111) plane is at an angle of $90 - \phi = \theta$ with the grain boundary. It is then seen in Figure 6 that the θ values for highest intensity of (111) reflections change from 25-45° near the surface to 55-70° at the center of the plate.

Robertson and Tetelman[1] have indicated that susceptibility of f.c.c.

*We wish to acknowledge the many helpful discussions concerning this phase of the project with Dr. L.P. Skolnick of the University of Maryland.

alloys undergoing intergranular corrosion is greatest when the (111) are oriented at 70° to grain boundaries which are normal to the stress direction as shown in Figure 8. The basis for this was theory by Stroh[2] which says that the normal stress σ acting on the grain boundary* making an angle θ with the slip plane is:

$$\sigma = 3/2 \left(L_o/r\right)^{1/2} \sigma_o \sin\theta \cos 1/2\,\theta$$

where σ_o = applied stress

L_o = length of slip plane occupied by a group of piled-up dislocations

r = crack length

θ = angle between slip plane and grain boundary.

Assuming L_o, r and σ_o constant, it can be seen that the normal stress acting on the grain boundary (or probability of cracking) is proportional to sin θ cos 1/2 θ. (σ_o was varied slightly in our tests, but not enough to account for the differences in susceptibility.)

Figure 9 is a plot of sin θ cos 1/2 θ against θ (the angle between slip planes and the grain boundaries. It is seen that the probability of cracking is greatest at 70°. Also shown on this graph are plots of average intensities of (111) vs. θ for the specimens taken from various levels within the plate. Average intensities for five degree angle ranges were taken from the X-ray data because of the highly fluctuating nature of that data. Figure 9 clearly indicates that stress corrosion susceptibility should increase with distance from the surface of the plate.

To see if this relation between depth and susceptibility exists as indicated by the preferred orientation studies, stress corrosion tests were run on subminiature tensile specimens, dimensions shown in Figure 10, machined from various depths of a 2.5 inch thick plate of 7075-T651 aluminum alloy. These were all electropolished to reduce the effects of machining. All but 1/8" of the gage length was covered with a protective rubber coating. Six (five in one case) specimens from each location were tested under constant load at 50% of yield strength in the Alcoa H solution. All specimens were tested at a constant temperature of 35°C, using the constant temperature equipment of Figure 5.

Failure times for each level in the plate are given in Table 1. The arithmetic mean of the failure times is given as is also a mean calculated

*Only grain boundaries normal to the applied stress are assumed important.

from the logarithms of the failure time. The mean based on the logarithm of endurance is believed to be a better way of comparing the endurance time because the logarithm of endurance is normally distributed as shown by Booth and Tucker[3].

Figure 11 shows the log mean endurance time and the range in data plotted against distance from plate surface. A statistical analysis of variance was performed on the data. At the 0.01 significance level, the conclusion was that the data were not from a homogeneous population. Therefore, the groups of specimens did differ significantly in the variability of their endurance times (i.e., the times to failure for the different groups were significantly different.)

On comparing the stress corrosion results with the mechanical properties shown in Figure 12, it can be seen that the mechanical properties cannot account for the differences in the stress corrosion endurance at the various levels on the plate. It was seen there that the mechanical properties remained nearly constant except at 3/8" from the surface, where the tensile properties were considerably higher.

However, on comparing the stress corrosion results with the preferred orientation results, Figure 13, it is seen that the preferred orientation predicts susceptibilities as observed (i.e., more susceptible toward the center) for all but the specimens taken from 3/8" below the surface of the plate. Figure 13 shows observed susceptibility as $(\text{endurance time})^{-1}$ and predicted relative susceptibility plotted against distance from the surface of the plate. It is expected that the curve for observed susceptibility would be of the same shape as that for predicted susceptibility if more specimens were tested between the 1 1/8" and 1 3/8" levels.

It is also believed that the group of specimens from 3/8" depth were more susceptible due to the stress level at which they were run. Since all specimens were run at 50% of Y.S., and the 3/8" level specimens had the highest yield strength, they were run at the highest level.

Role of Direction for a Fixed Depth: Besides the effect of depth for a given direction, further examination of Figure 6 shows that at a given depth (the plate interior) the preferred orientation results would predict the susceptibilities as: short transverse > long transverse > longitudinal. It can be seen that for the short transverse stress direction (normal to plane of pole figure) the intensity of reflections from favorably oriented (111) is greatest and for the longitudinal stress direction (same as rolling direction shown) the number of favorably oriented (111) planes is least. For the long transverse stress direction (in the plane of the pole figure, but normal to the rolling direction), the number of favorably oriented (111) plane is seen to be between that for the short transverse and longitudinal directions. Therefore, the number of favorably oriented slip planes might be used to predict the relationship between susceptibility and orientation.

Whether this prediction holds or not will be tested in future work.

The Role of Segregation in the Susceptibility of 7075

Electron probe microanalyses were made of 7075-T651 and -T73 material. Specimens were taken perpendicular to the rolling plane from the center and from near the surface of the plate. At each level, specimens were taken both perpendicular and parallel to the rolling direction.

The target current images of areas with inclusions are shown in Figure 14 for the specimens near the surface of both the 7075-T6 and -T73 conditions. The light areas indicate inclusions of lower atomic number and the dark indicates inclusion of higher atomic number than the matrix. In Figure 15, the magnesium X-ray images, the light areas are high in magnesium content. These areas correspond to the light particles in Figure 14 and, as determined by other X-ray images, are also high in silicon. It was also determined that the dark inclusions of Figure 9 were low in magnesium and silicon.

Figure 16, the iron X-ray images, shows iron to be highly segregated at the dark particles of Figure 14. Copper and manganese were also segregated at these inclusions. Aluminum and zinc were found to be depleted at all inclusions.

The chromium X-ray image, Figure 17, shows that there are zones depleted of chromium that do not correspond to the inclusions of Figure 9.

Titanium, not shown, also follows the chromium. These depleted zones are seen to be more prominent in the 7075-T651 than in the -T73 material and are believed to correspond to subgrain boundaries and may explain the higher susceptibility of 7075-T651. Further investigation will be made to try and correlate these depleted zones directly with the grain or subgrain boundaries.

The only difference found in the electron probe microanalysis between the material from the center and from near the surface of the plate was that approximately twice the magnification was required for the specimens from near the surface in order to see inclusions of the same size as near the center. This is believed to be due to the more highly deformed nature of the material near the surface. The significance of this segregation of different constituents as a function of directionality will be explored more deeply by the electron probe technique in future work.

TABLE 1

STRESS CORROSION ENDURANCE TIME AT VARIOUS LEVELS

IN A PLATE OF 7075-T651 ALUMINUM ALLOY

Distance from Surface *(in.)	Mean Endurance Time (min.)	Log Mean Endurance Time **(min.)
3/8	4.66	4.57
5/8	11.91	11.40
7/8	9.63	8.74
1 1/8	7.07	6.82
1 3/8	5.02	4.97

*Distance from surface is distance to center of 1/4" gage length specimens. Six specimens were run from all but the 3/8" level where five were run.

**Log mean endurance time is the anti-logarithm of the mean of the logarithms of the times to failure.

REFERENCES

1. Robertson, W.D. and A.S. Tetelman, Strengthening Mechanisms in Solids, ASM, p. 217 (1960).
2. Stroh, A.N., Proc. Roy. Soc., 223, 404 (1954).
3. Booth, F.F. and G.E.G. Tucker, Corrosion, Vol. 21, p. 173 (1965).

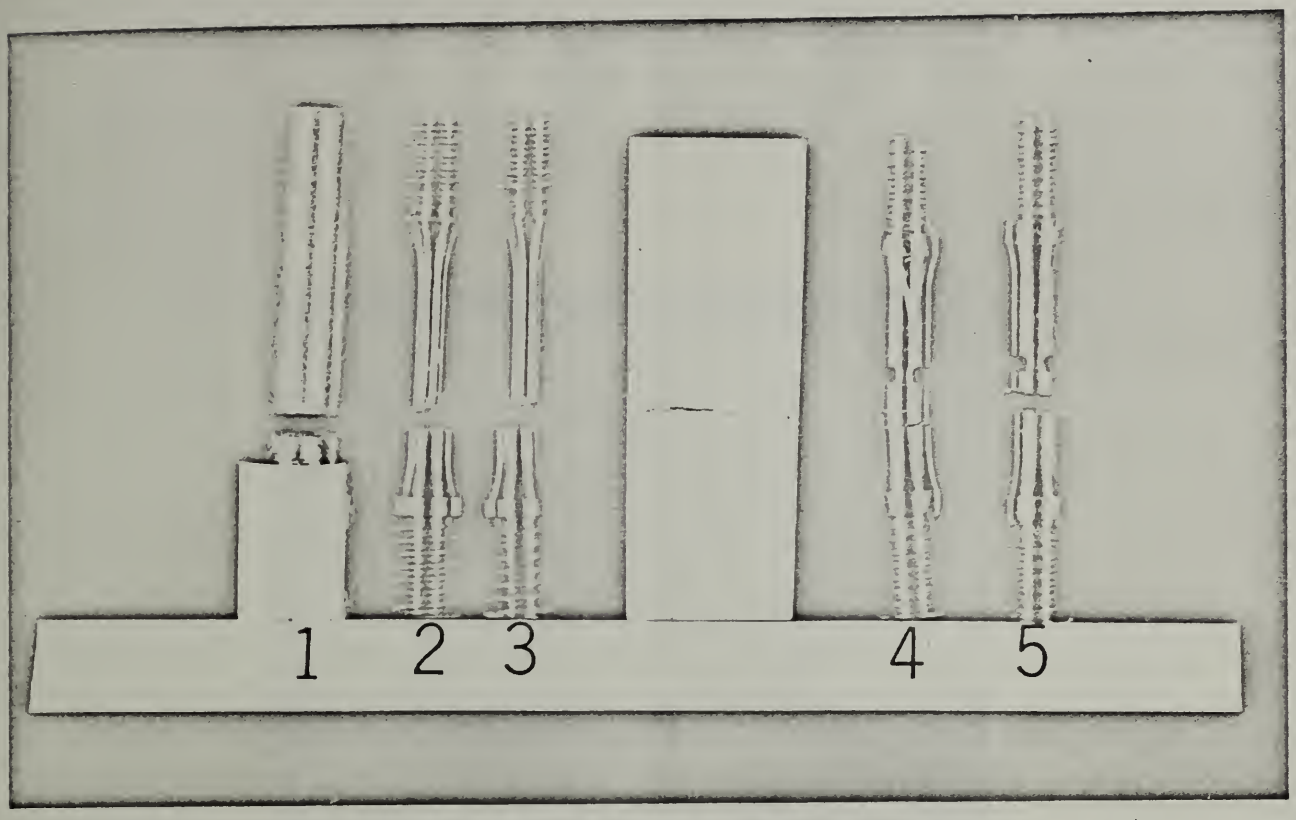

Figure 1

2219-T87 aluminum alloy short transverse specimens, 1, 2 and 3 broke during machining. Specimens 4 and 5 broke in tensile test at a region 9/4 the area at the root of the notch. The cross-section of the plate was etched with Flick's reagent. X 1

Figure 2

End of 7075-T6 extrusion perpendicular to extrusion direction showing grain flow. Piece shown is 3" x 4". Die size was 3" x 6". 1, 2 and 3 show areas of specimen extraction for photomicrographs in Figure 4. Etched in Flick's reagent. X 1

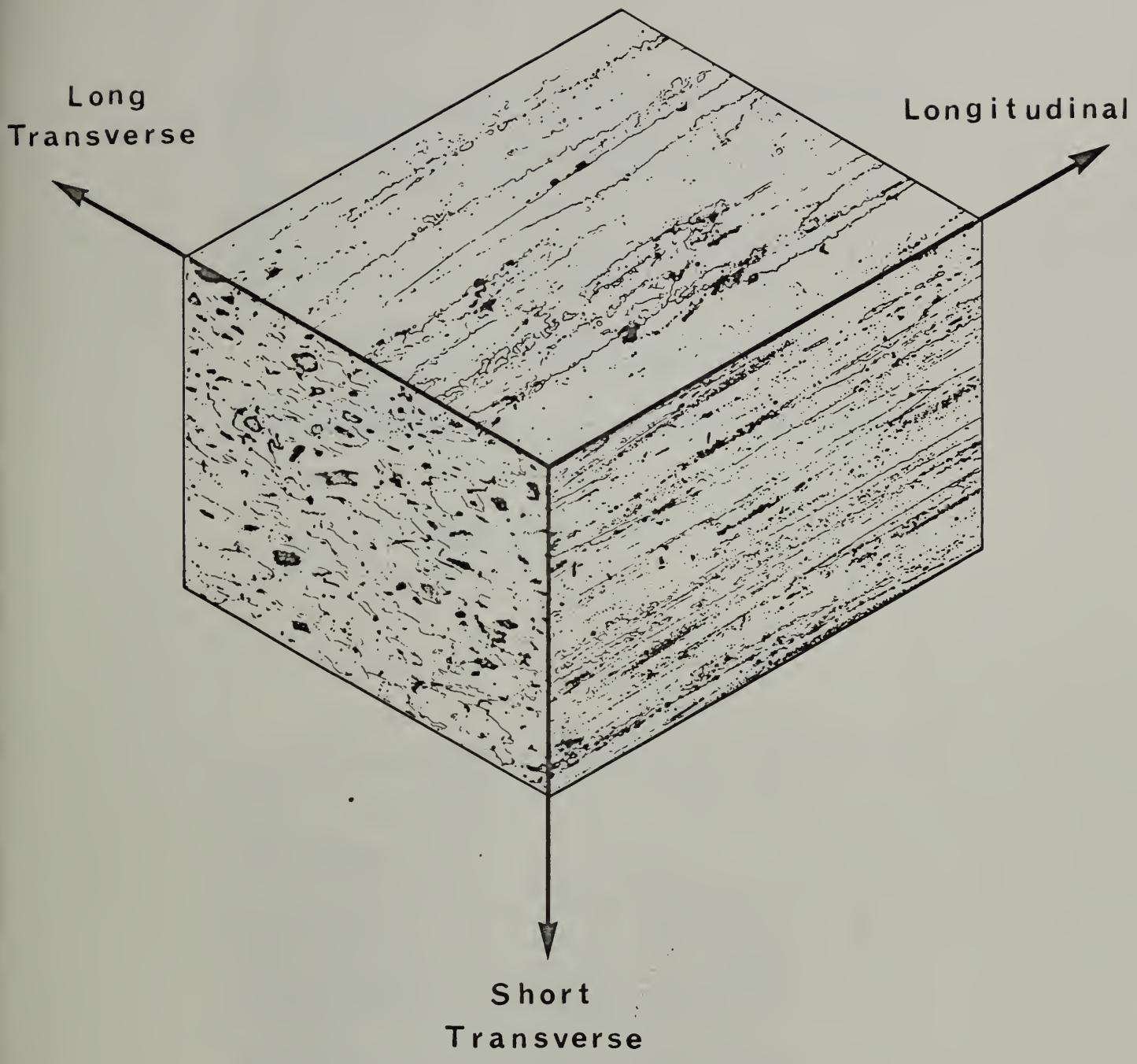

Figure 3

Composite micrograph illustrating the grain structure in three orientations at the center of a 7075-T6 aluminum alloy extrusion. Die size 3" x 6". Specimens taken from area at center of block shown in Figure 2. Etched in Keller's etch. X 100

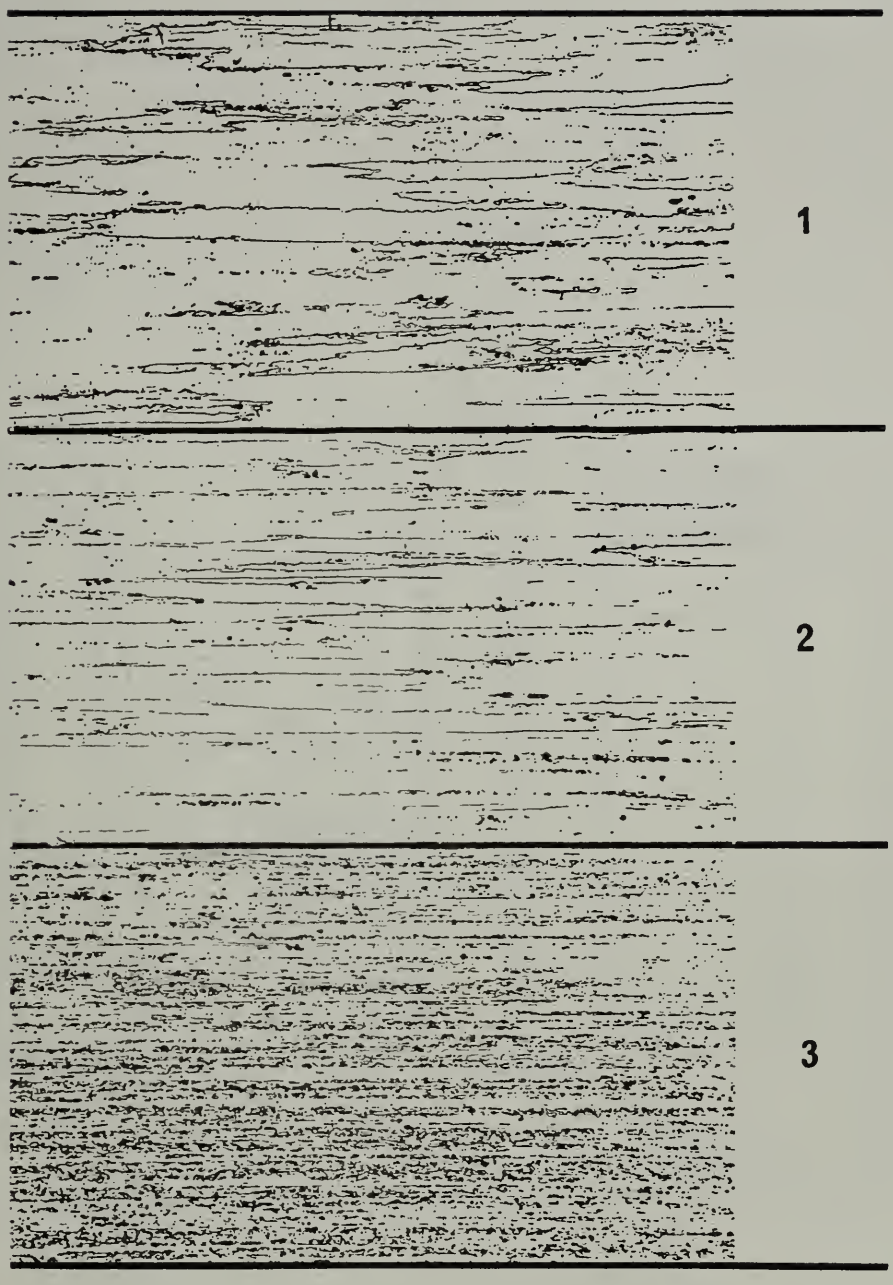

Figure 4

Photomicrographs showing the change in grain structure in the plane perpendicular to the short transverse direction with distance from the die surface in a 7075-T6 aluminum alloy extrusion. Specimens taken from areas 1, 2 and 3 shown in Figure 2. Keller's etch. X 50

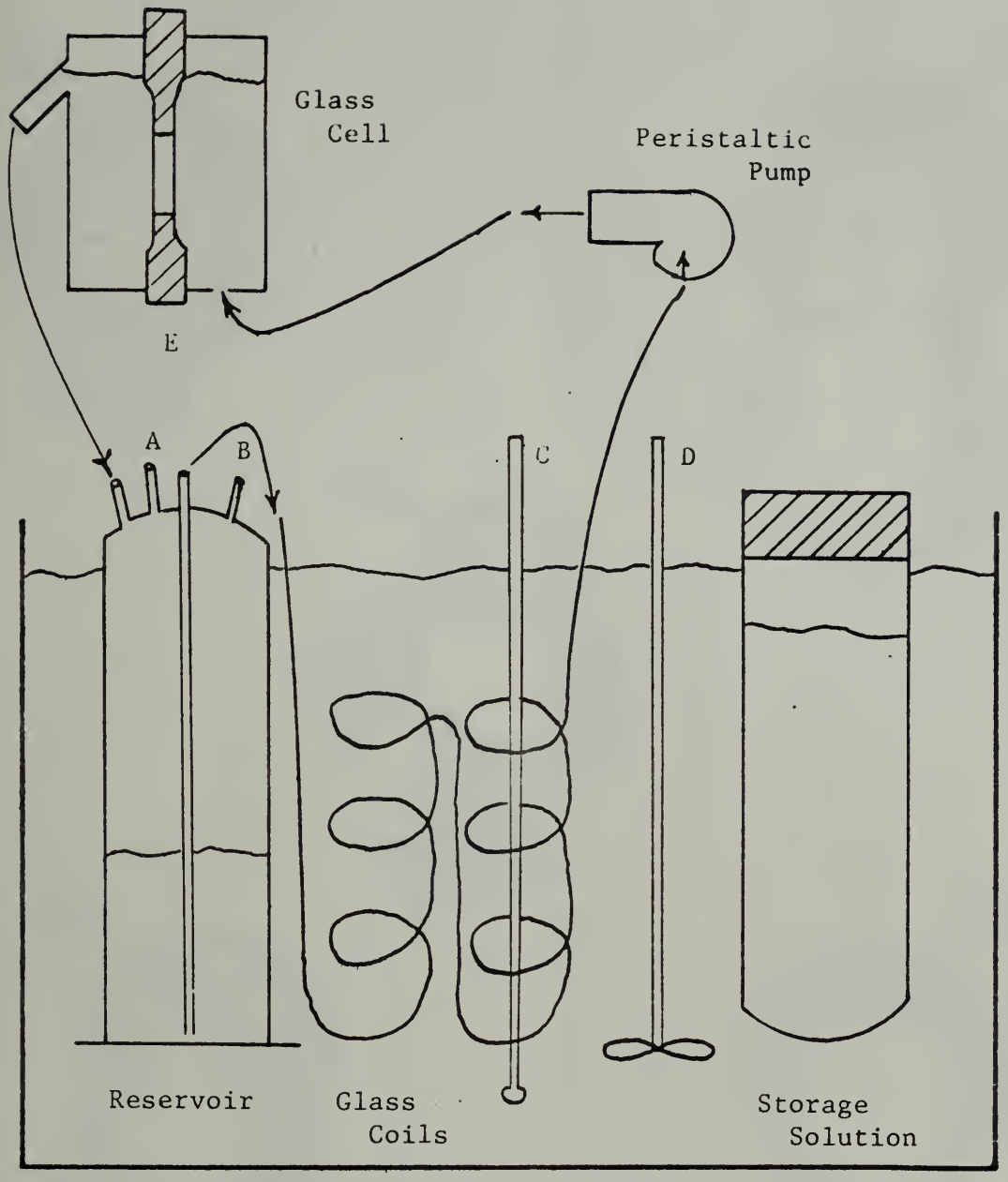

KEY

A	Fill Vent
B	Fill Hole
C	Bath Thermometer
D	Stirer
E	Miniature Specimen

Figure 5

Constant temperature stress-corrosion testing system showing flow of corrosive solution.

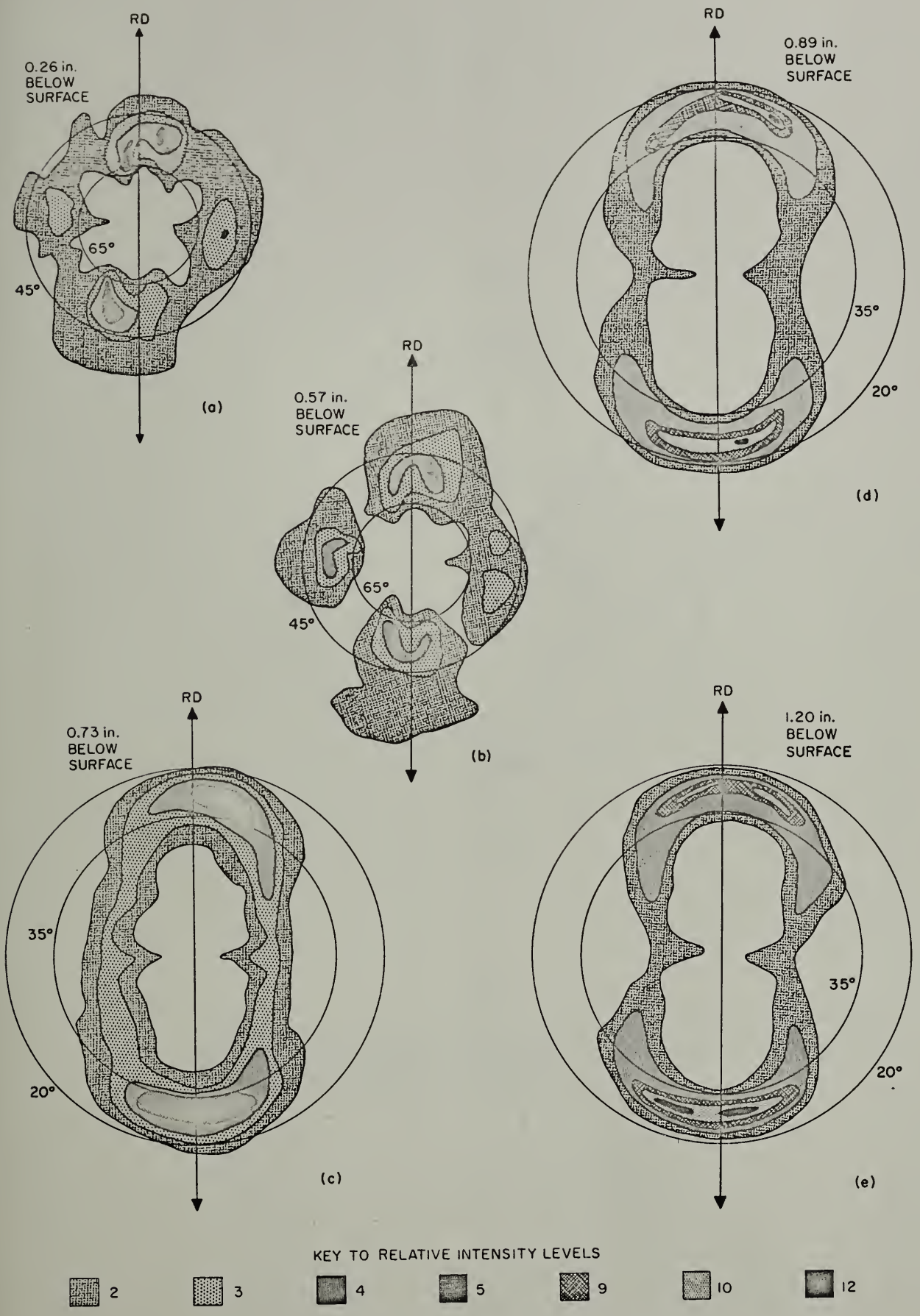

FIGURE 6: (III) - POLE FIGURES OF SPECIMENS PARALLEL TO THE SURFACE OF A 2.5 in. THICK 7075-T651 ALUMINUM ALLOY PLATE.

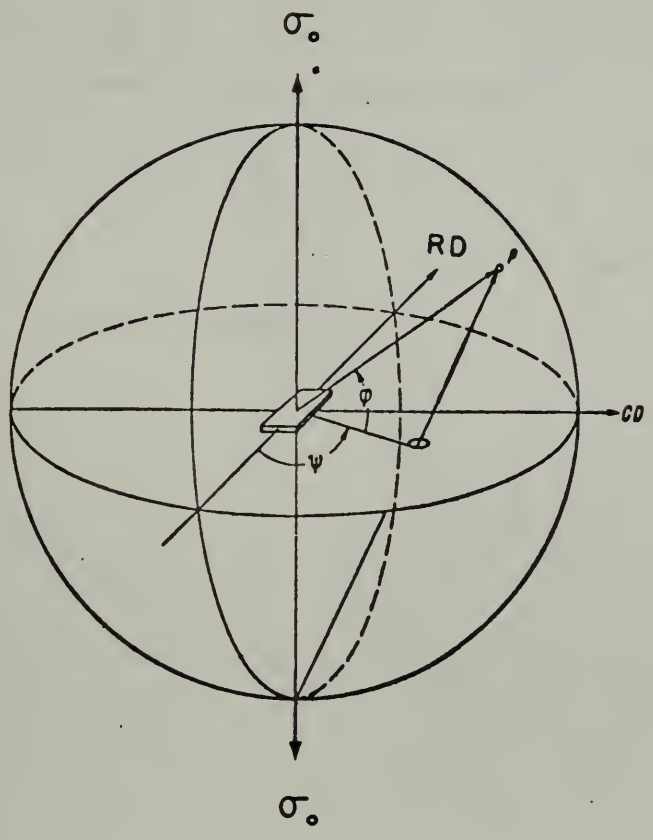

Figure 7

Representation of lattice places of a rolled metal specimen in stereographic projection. The equator plane was chosen as the plane of projection.

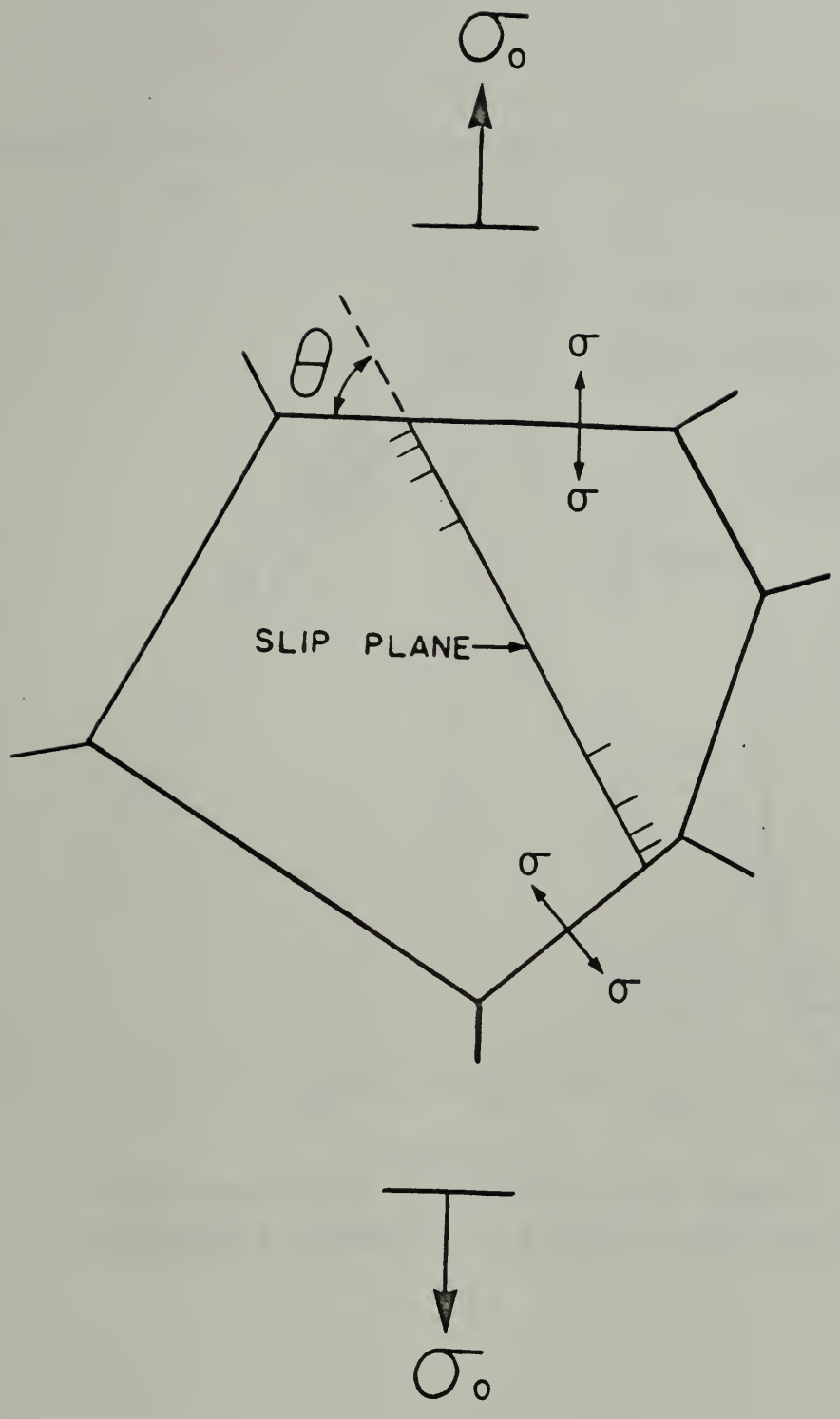

Figure 8

The stress normal to the grain boundary, σ, is maximum when both the grain boundary is normal to the applied stress and the stress due to dislocations piled up is greatest. The stress due to piled up dislocations is greatest when the slip plane is at an angle of $\theta = 70.5°$ to the grain boundary.

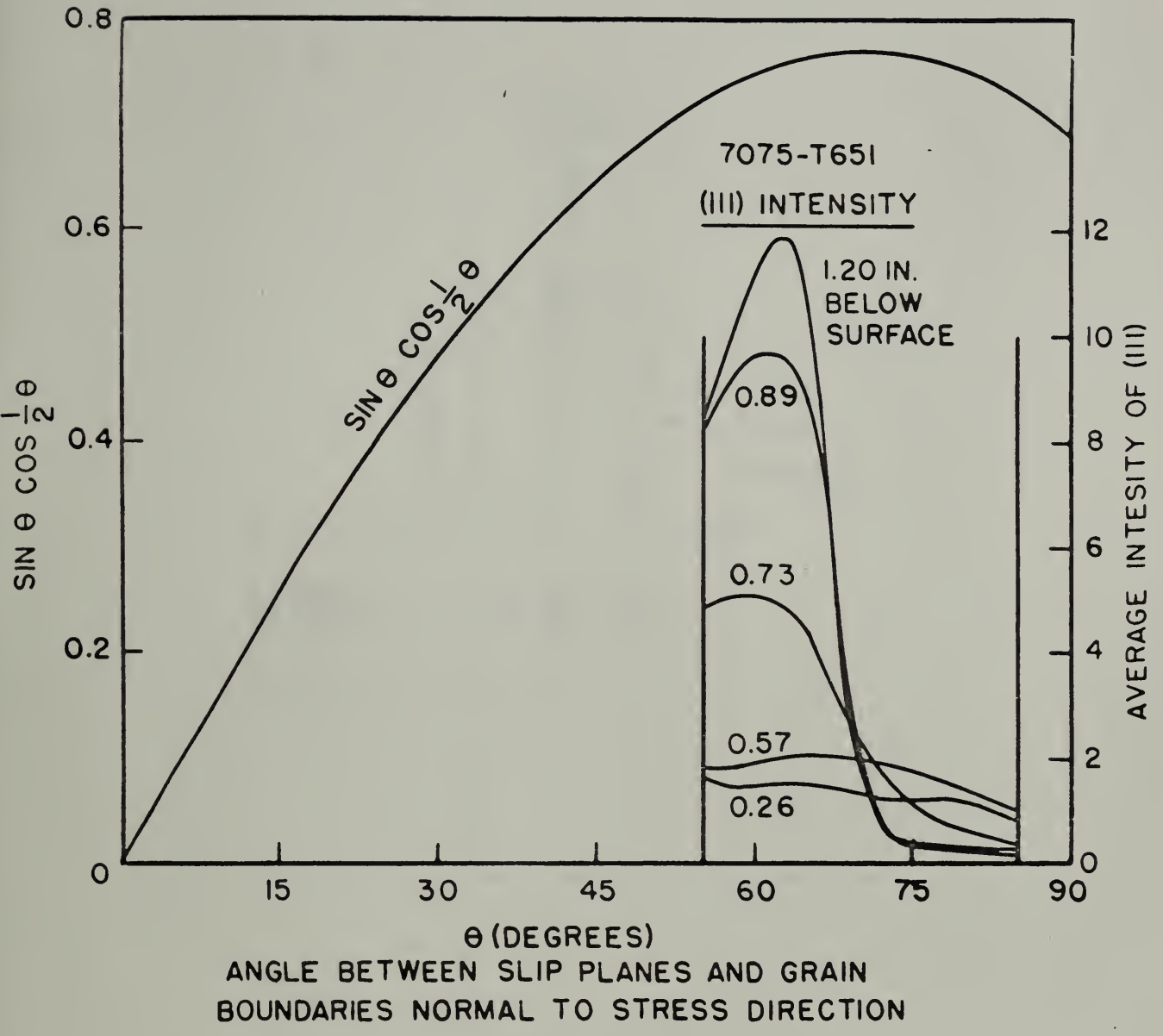

Figure 9

The probability of cracking is shown plotted against the angle between slip planes and grain boundaries normal to the applied stress. Superimposed on this are plots showing the intensity of (111) reflections at various depths in a 7075-T651 aluminum alloy plate. The intensity of (111) reflections in the range from θ = 55 to 85° is a measure of the number of (111) favorably oriented for stress corrosion cracking.

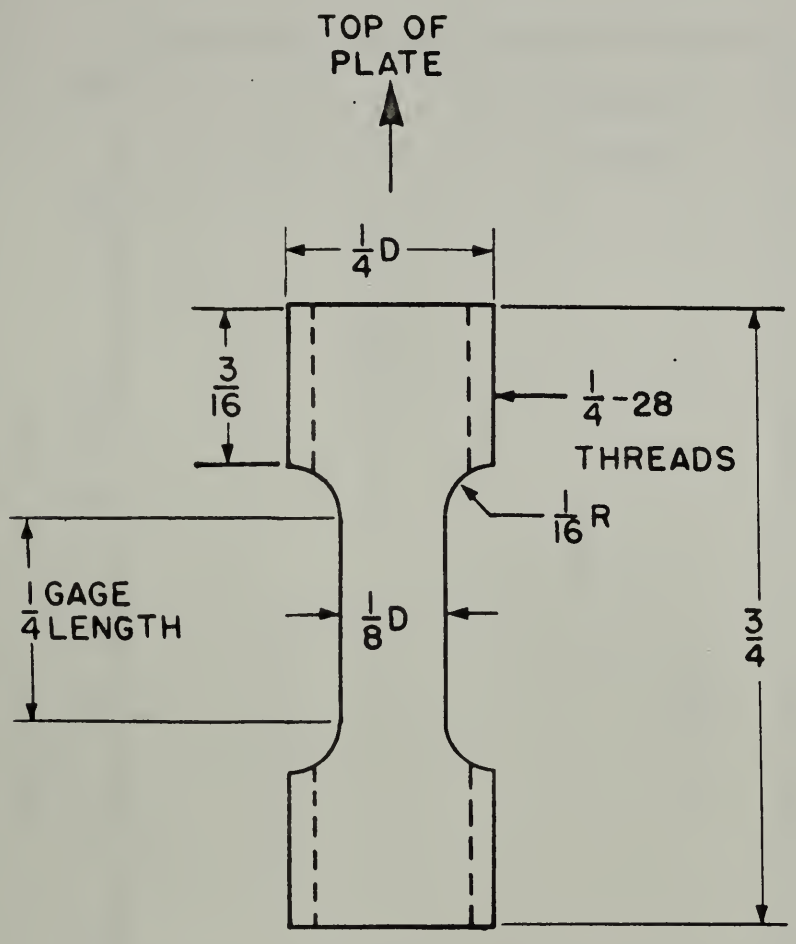

Figure 10

Dimensions of subminiature round tensile specimens used to determine the susceptible to stress corrosion cracking at various depths in a plate of material.

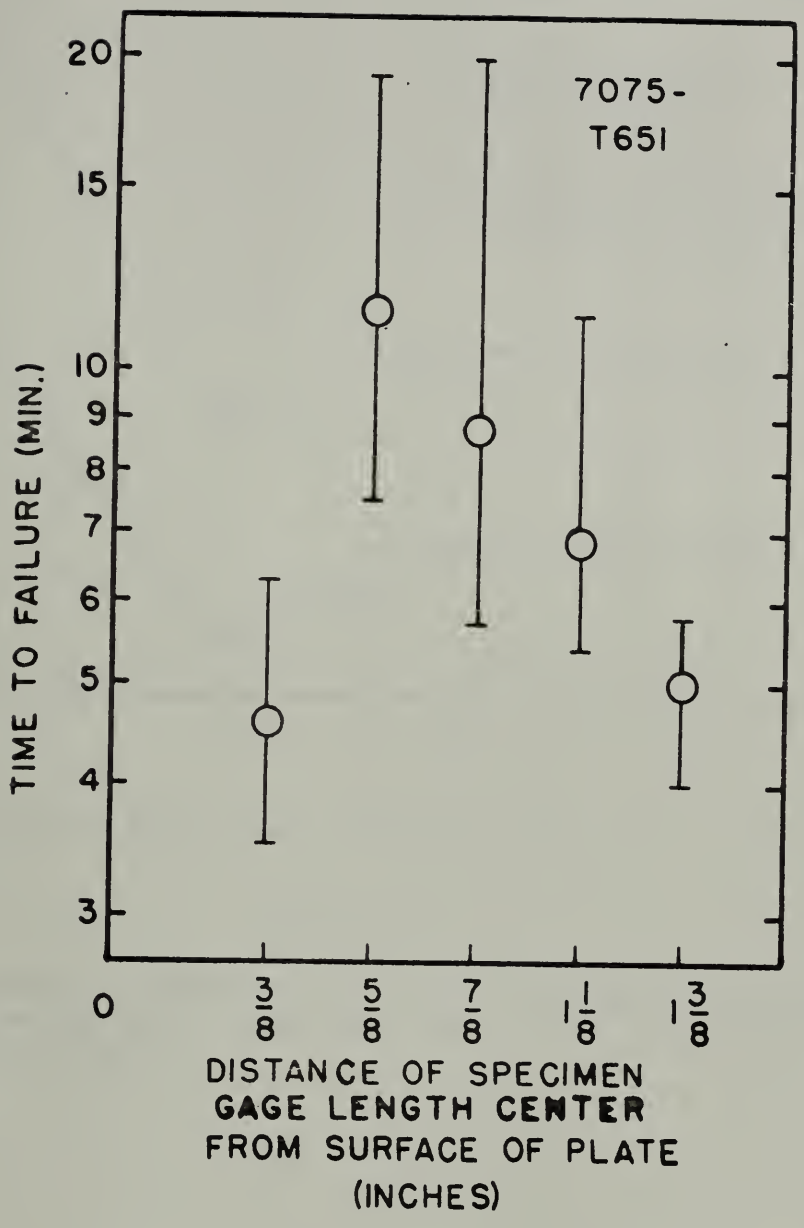

Figure 11

The stress corrosion endurance of short transverse specimens is shown at various levels of a 7075-T651 aluminum alloy plate. Both the log mean endurance time and the range in data are shown.

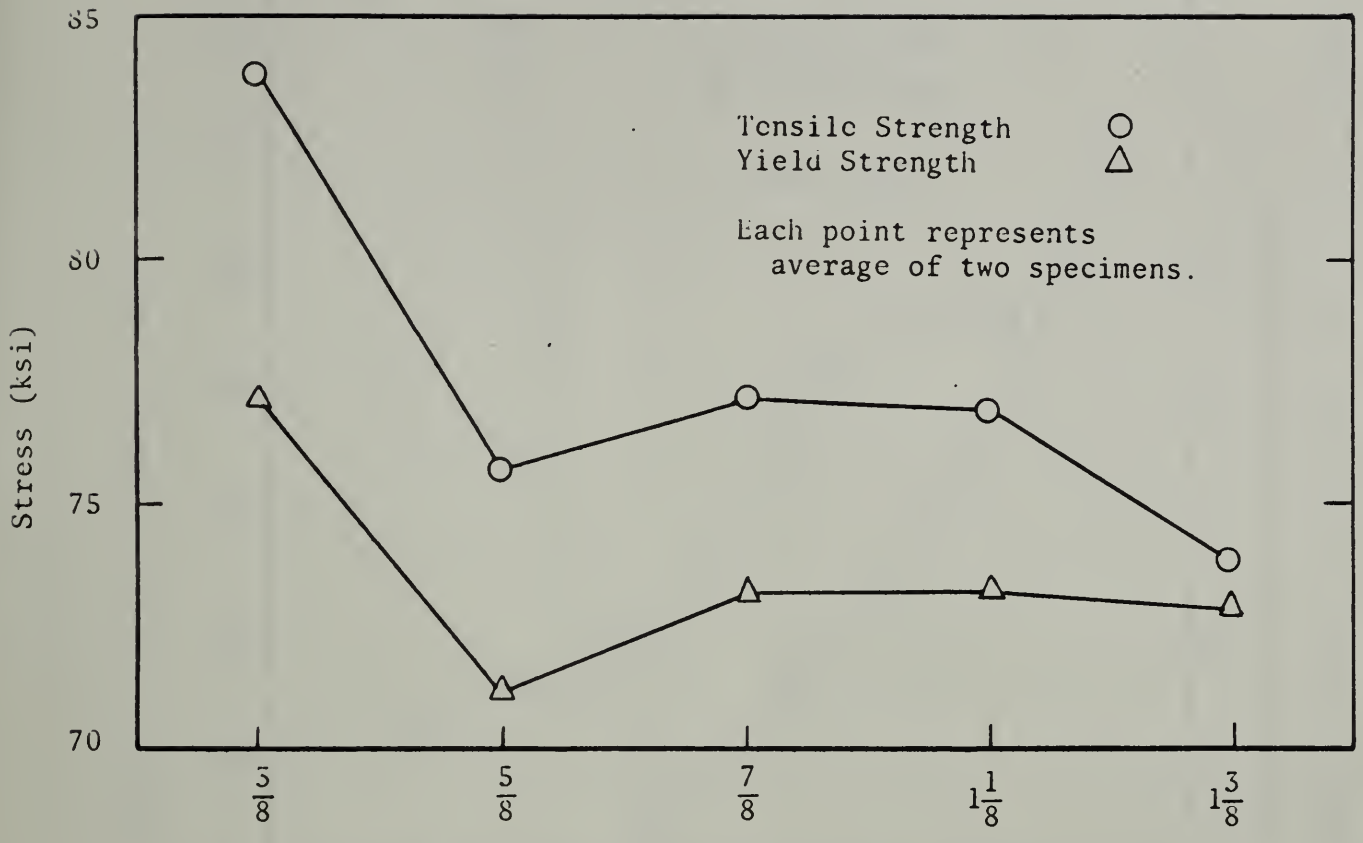

Figure 12

Mechanical properties of short transverse 7075-T651 aluminum alloy specimens versus depth in a 2.5 in. thick plate.

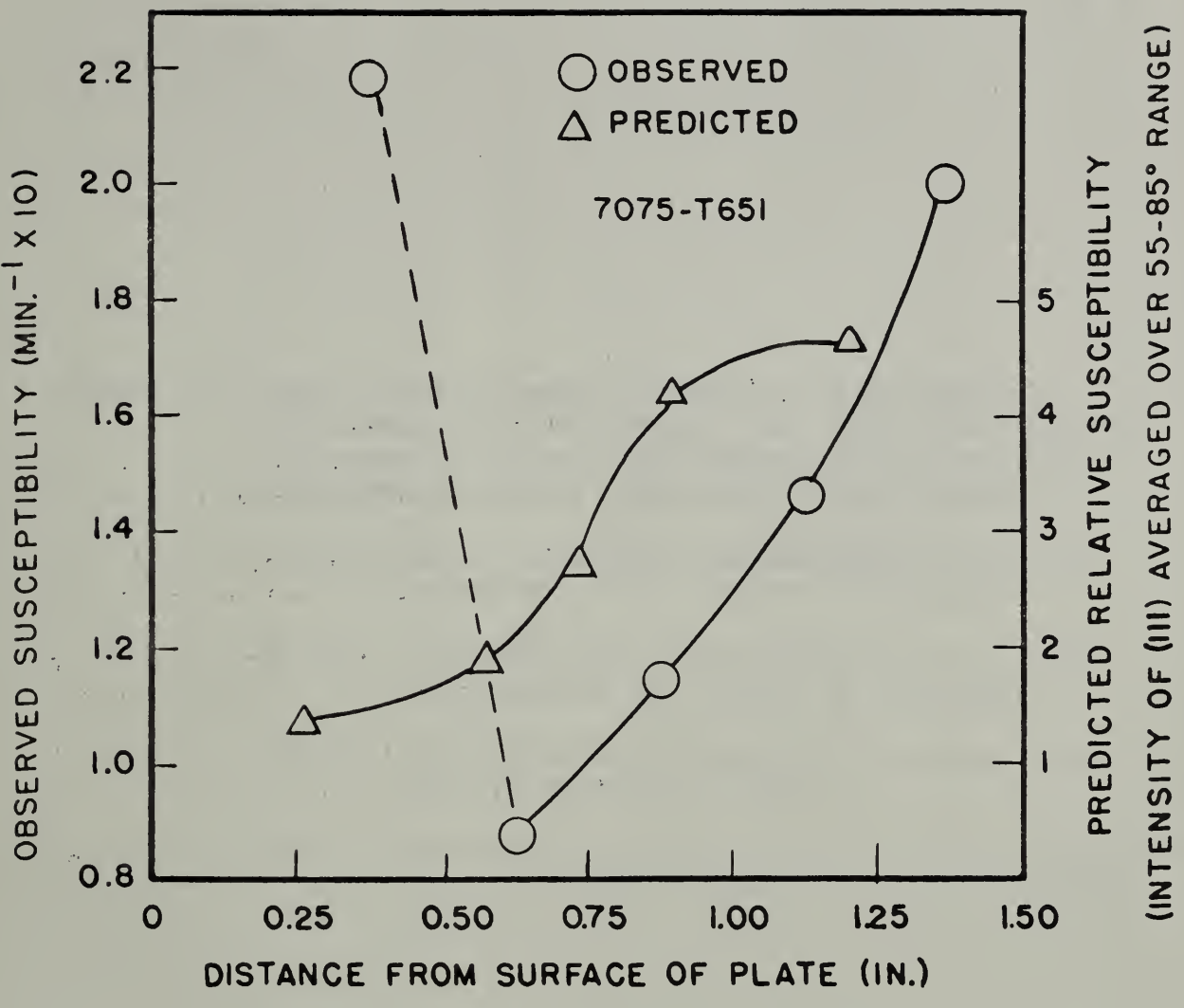

Figure 13

The observed stress corrosion susceptibility and the predicted susceptibility are shown plotted against distance from the surface of a 7075-T651 aluminum alloy plate.

Figure 14. Target current images of areas of 7075 aluminum alloy plate with inclusions. The light areas indicate inclusions of lower atomic number and the dark areas, inclusions of higher atomic number than the matrix.

T73-1S. 7075-T73 material perpendicular to rolling direction, at the surface of the plate.

T6-1S 7075-T651 material perpendicular to rolling direction, at the surface of the plate.

T73-2S 7075-T73 material parallel to rolling direction, at surface of plate.

T6-2S 7075-T651 material parallel to rolling direction, at surface of plate.

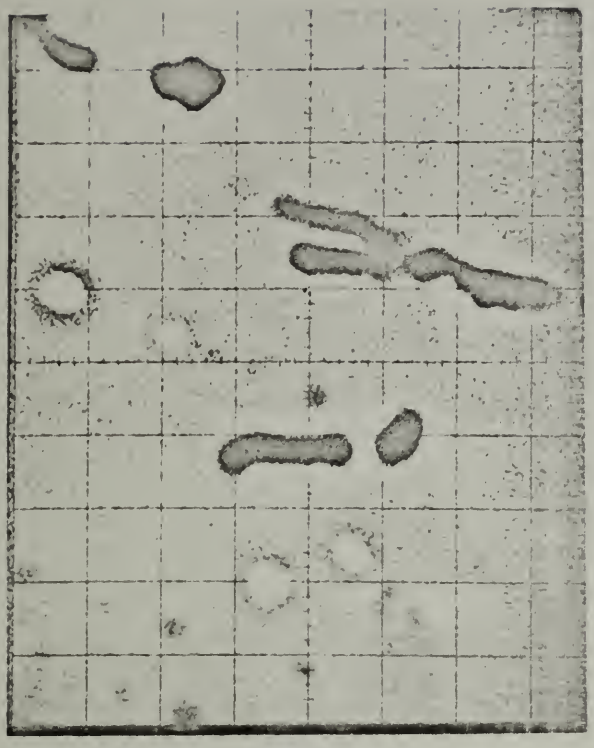

T6–1S

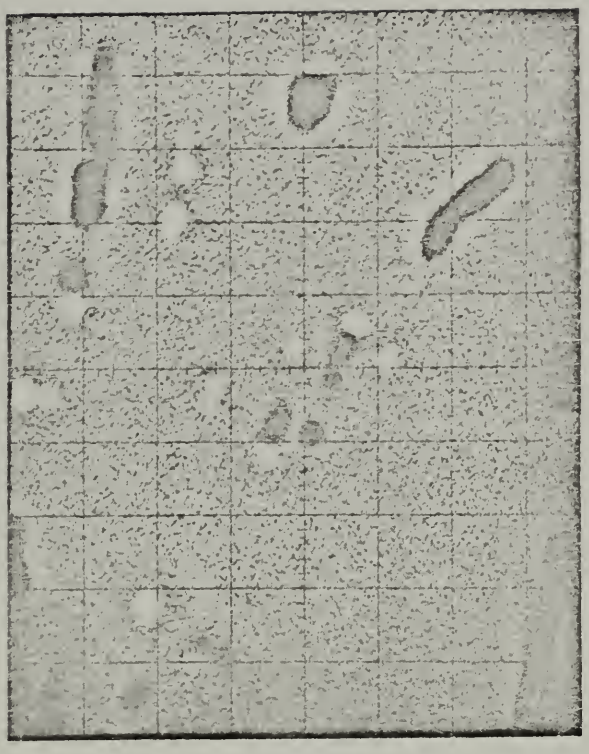

T6–2S

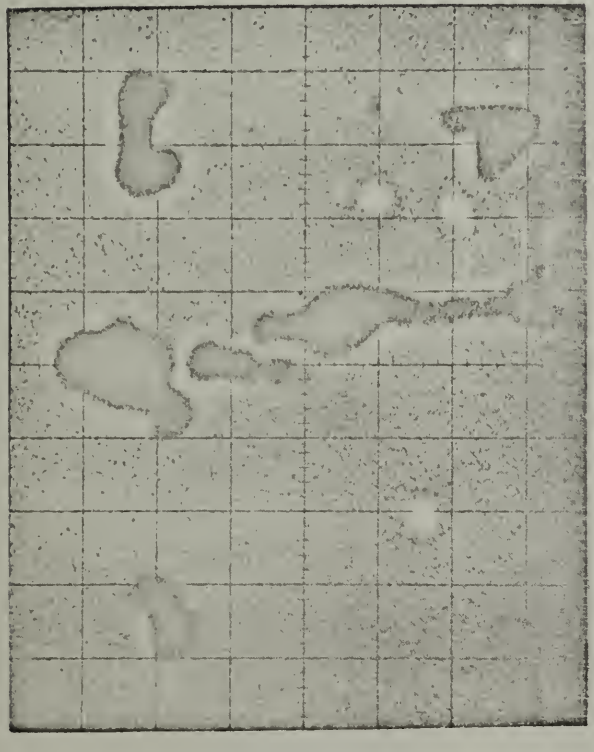

T73–1S

T73–2S

TARGET CURRENT IMAGES 7μ/div.

Figure 15. Magnesium X-ray images of areas shown in Figure 14. Light areas are high in magnesium.

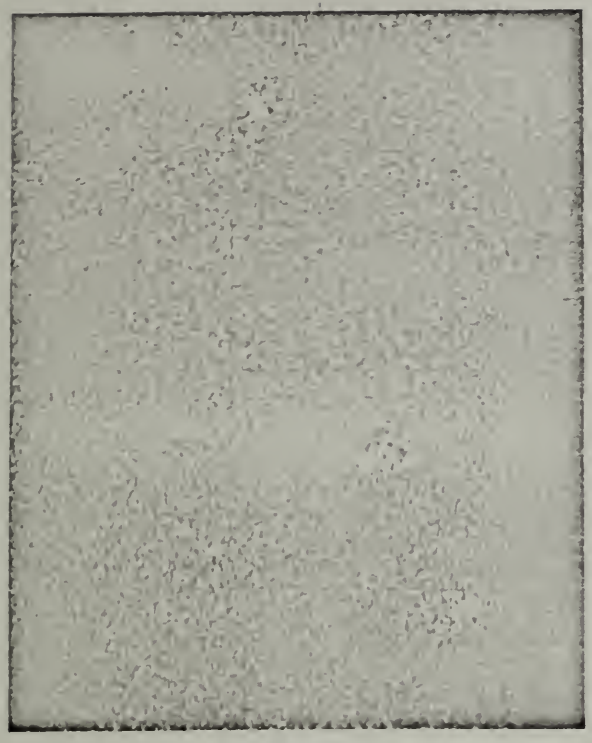

T6-1S

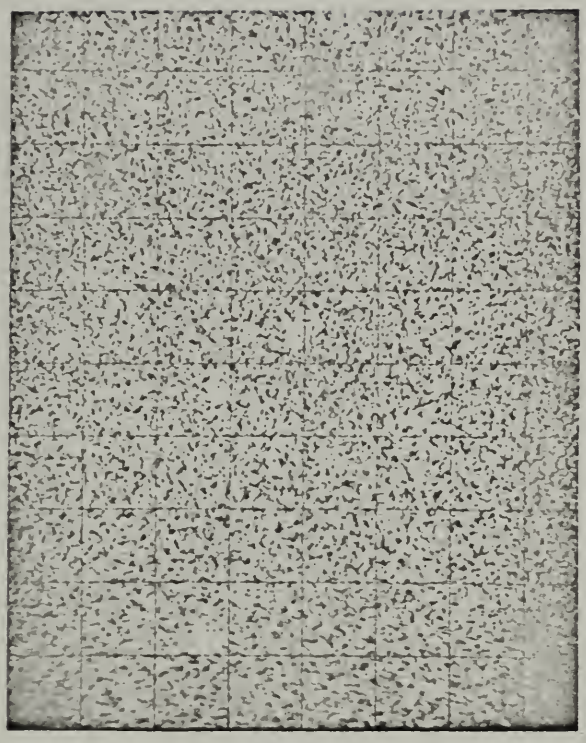

T6-2S

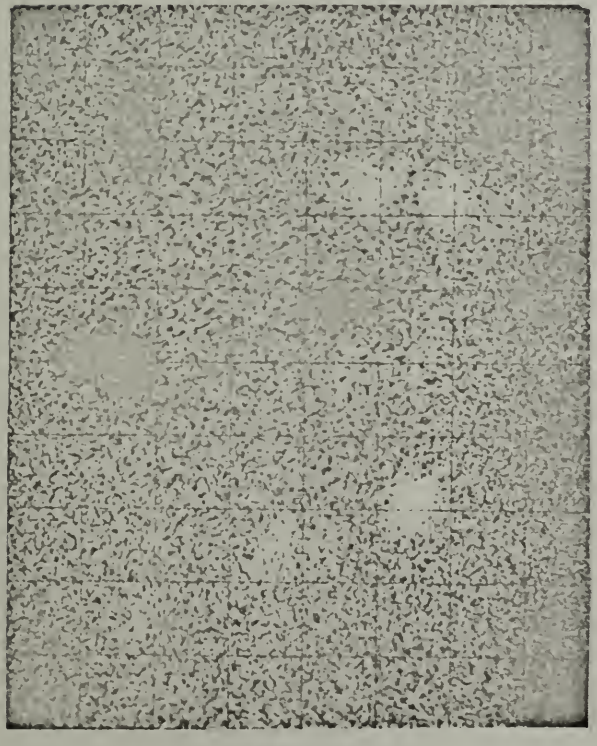

T73-1S

T73-2S

MAGNESIUM X-RAY IMAGES

Figure 16. Iron X-ray images of areas shown in Figure 14. Light areas are high in iron.

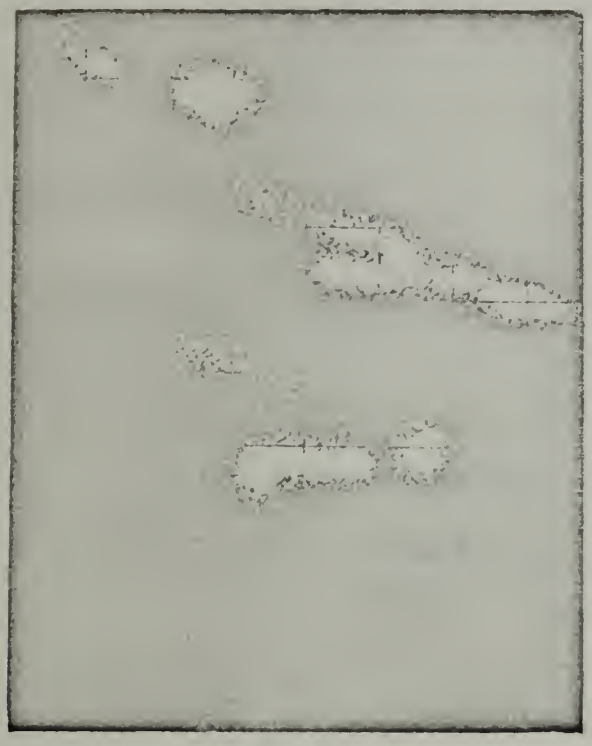

T6-1S

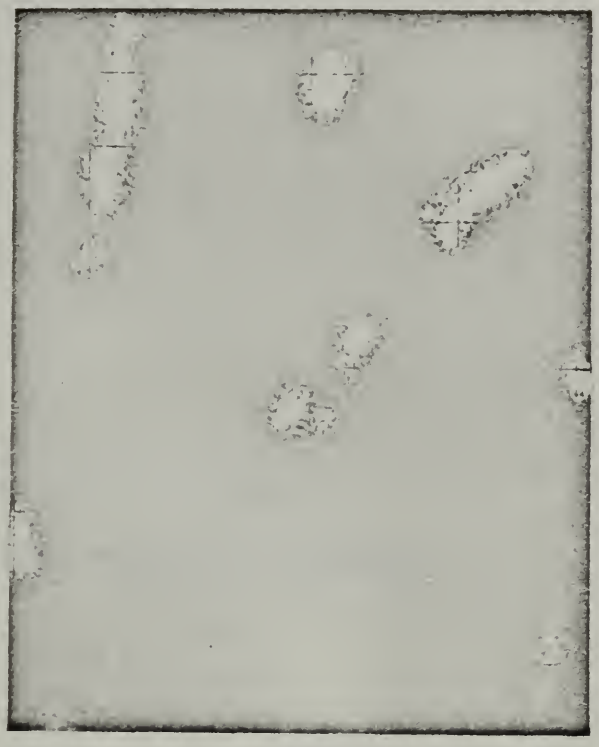

T6-2S

T73-1S

T73- 2S

IRON X-RAY IMAGES

Figure 17. Chromium X-ray images of areas shown in Figure 14. Light areas are high in chromium.

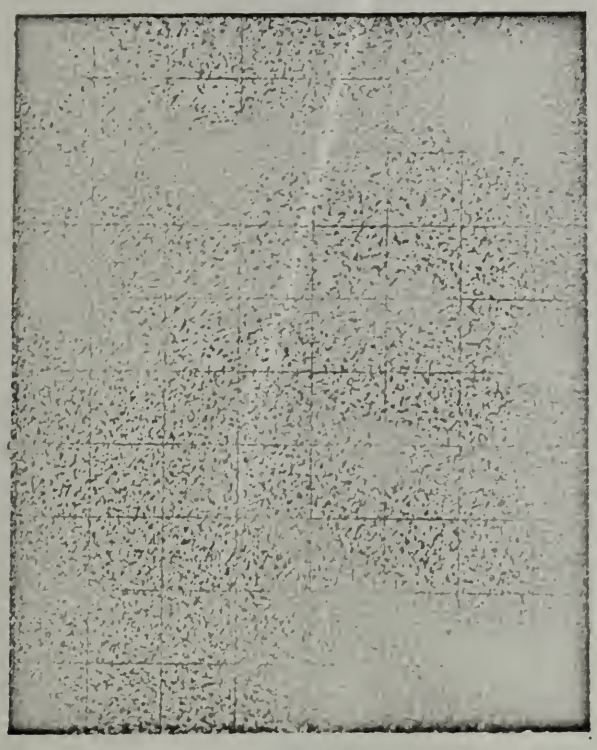

T6–1S

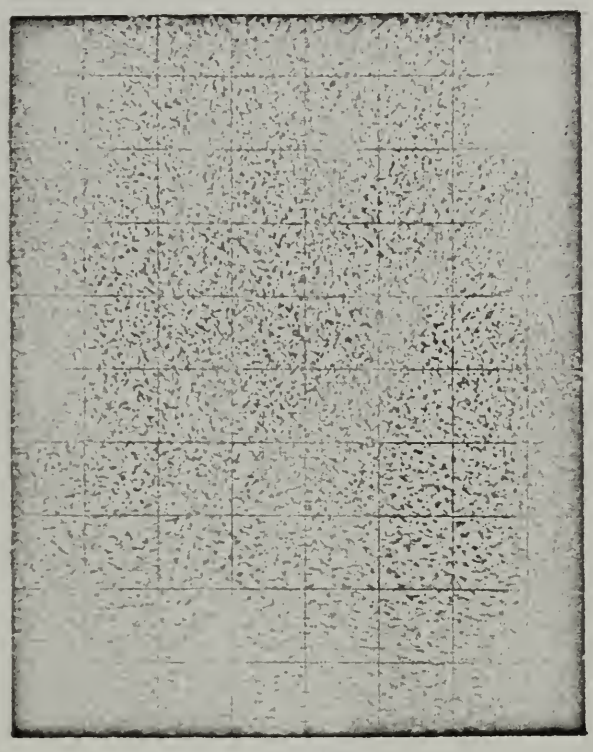

T6–2S

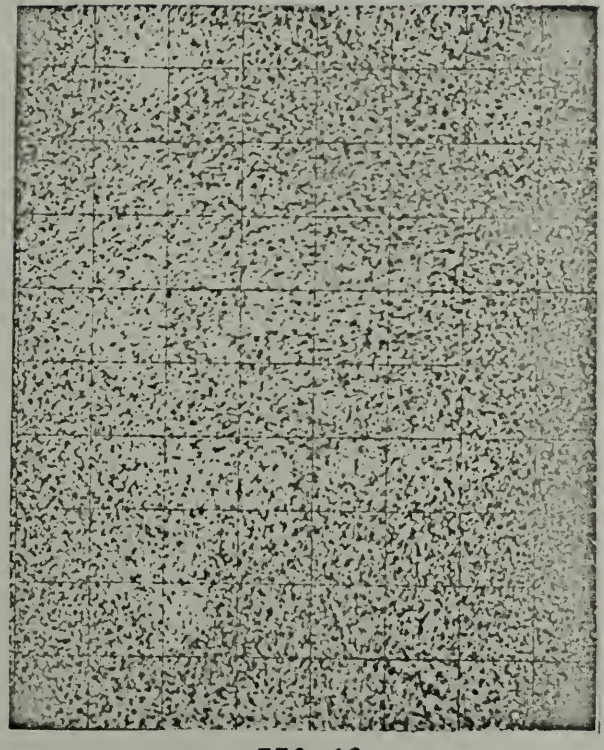

T73–1S

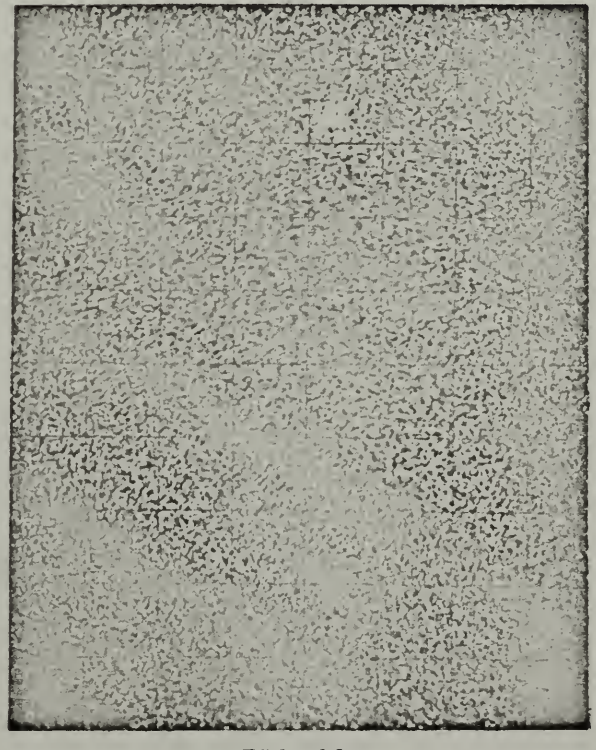

T73–2S

CHROMIUM X–RAY IMAGES


DEPARTMENT OF COMMERCE
NATIONAL BUREAU OF STANDARDS